Adaptive Multiplexed RT-PCR Assay for Detection of Chikungunya, Dengue, and Zika Viruses

By

Erin Marie Euliano

Thesis

Submitted to the Faculty of the

Graduate School of Vanderbilt University

in partial fulfillment of the requirements

for the degree of

MASTER OF SCIENCE

in

Biomedical Engineering

May 11, 2018

Nashville, Tennessee

Approved:

Frederick Haselton, Ph.D.

Nicholas Adams, Ph.D.

ACKNOWLEDGMENTS

Thank you to Dr. Rick Haselton and Dr. Nick Adams for your unwavering support over the last few years – it has meant the world to me. Thank you to Dr. Bill Gabella for teaching me LabVIEW and keeping me company in the lonely Adaptive PCR room, even with your weird music. Thank you to Megan Pask for your organization and endless knowledge and kindness – you have made my time here much easier. Thank you to all other members of the Haselton Lab for all your help and friendship.

Thank you to my family and friends for supporting me through these crazy two years. Suite 1303 (actual and honorary residents) – you keep me sane. Thank you for putting up with me. Niki and Leah, I adore you. Mom, Dad, Matt, and Catherine – you're the best. I love you.

Last but certainly not least, I would like to thank my Savior Jesus Christ, without whom none of this work would have been possible.

TABLE OF CONTENTS

Page

LIST OF TABLES

Table Page

LIST OF FIGURES

Figure Page

1: INTRODUCTION

1.1 The Global Health Importance of More Versatile Viral Diagnostics

Mosquito-borne viruses kill approximately 725,000 people per year as estimated by the World Health Organization (WHO), making mosquitoes the deadliest animal in the world. The *Aedes aegypti* mosquito in particular can transmit dengue, Zika, and chikungunya viruses, among others. All three can express as fever, muscular pain, conjunctivitis, and headache, but each can be accompanied by a different long-term consequence. Dengue fever can lead to life-threatening Dengue Shock or Dengue Hemorrhagic Fever, chikungunya has been associated with persistent arthritis, and Zika virus has been the subject of recent serious health concerns as it has been linked to microcephaly when an expectant mother is infected during the first trimester (1-8).

If someone who lives in or has recently visited an area where these viruses are endemic presents with symptoms like those mentioned above, the Centers for Disease Control and Prevention (CDC) and the WHO recommend informing their primary care physician and treating the symptoms (2-4, 6). In the absence of a confirmed diagnosis, the patient is instructed to get plenty of rest and drink fluids to prevent dehydration but is strictly warned against taking ibuprofen or other non-steroidal anti-inflammatory drugs (NSAIDs) until a dengue infection has been ruled out. NSAIDs interfere with the function of platelets, increasing the risk of uncontrolled bleeding; dengue infections cause a very low platelet count which, when combined with NSAIDs, greatly increases the risk of excessive bleeding or shock (9). Dengue Hemorrhagic Fever (DHF) and Dengue Shock Syndrome (DSS) can both be fatal, and no specific therapy exists, but a health care provider can use fluid replacement therapy if the patient is diagnosed and hospitalized early (2). In contrast, the symptoms of those with chikungunya tend to resolve after a week, although joint pain can persist (6). Zika symptoms are similarly mild and resolve fairly quickly, although if the

patient is a woman of child-bearing age, she should be tested immediately, as it has been heavily connected to microcephaly, a fatal birth defect (4). There have been cases reported in several countries of co-infections with chikungunya and dengue virus in the same patient (10); what is believed to be the first case of simultaneous infection with all three viruses was reported in Colombia in 2016 (11). Without diagnostic tools to identify which virus has infected a patient, proper treatment or patient management cannot be administered, increasing the risk of adverse outcomes.

While molecular methods of detecting infection by specific viruses have been in use for years (12), these techniques have not been utilized to their full potential in the developing world. Clinics in these low-resource settings have little-to-no laboratory support, precluding the use of high end diagnostics. In this void, clinical diagnoses are most commonly determined based on symptoms; such analyses, however, can be unreliable and nonspecific, as many viral and bacterial infections present very similarly. This causes confusion in symptom-based diagnostics and can result in increased mortality (13). Undiagnosed and untreated communicable diseases continue to be transmitted to others, making it much more difficult to contain outbreaks (14). Additionally, many illnesses and deaths in resource-limited areas go uninvestigated, so the full burden of individual diseases remains unknown.

1.2 Current Diagnostic Techniques Do Not Address the Needs in Low Resource Settings

Many devices developed to perform well in central laboratories are not well-suited for point-of-care clinics. According to the WHO, a diagnostic for use at the point-of-care in low-resource regions of the world must be affordable, sensitive, specific, user-friendly, rapid and robust, equipment-free, and deliverable to end users, abbreviated as “ASSURED” (15). There are

often tradeoffs between these criteria that must be mediated depending on the target users, e.g. increased speed may decrease affordability or improved portability may decrease sensitivity.

The primary methods of diagnosis for Zika recommended by the CDC are a test for detecting antibodies against Zika and a test for detecting Zika virus nucleic acids in the patient's blood or urine (16). Antibodies are formed as the body attempts to fight off a virus in the days and weeks after infection, making the former method less useful for early-stage detection. Viral nucleic acid sequences can be found in the patient during infection, making this method much more successful. Specific RNA or DNA fragments are detected through nucleic acid amplification by producing enough copies of the sequence that it is distinguishable from the background. All amplification techniques have a lower limit of nucleic acid concentration at which they produce results; for optimal virus detection, this limit should be lower than the normal amount of virus present in a patient sample, or the viral load.

A group in Thailand found that the median viral load of symptomatic chikungunya patients was on the order of 100 RNA copies per µL of patient sample, such as blood or urine, while asymptomatic patients showed loads on the order of 1 RNA copy per µL (7). A "very low viral load" for dengue virus, meanwhile, was considered to be 1 RNA copy per µL by the Bernhard Nocht Institute for Tropical Medicine in Hamburg, Germany (17). According to the WHO, the average viral load in a review of several studies on Zika infections is on the order of 10 RNA copies per µL in blood and 1 RNA copy per µL in serum (18).

Nucleic acid amplification (NAA) is considered to be the most specific and sensitive method for detecting viral infection, but the reaction requires precise conditions and laboratory training. Attempts have been made to develop an NAA device that meets the ASSURED criteria, but to date none have been successful (19). For example, the GeneXpert (Cepheid Inc. Sunnyvale,

CA, USA) uses NAA and a sample prep cassette to purify and detect tuberculosis DNA from a sputum sample. While early testing showed that it could be very effective in the developing world, tests in tropical regions report high failure rates due to high ambient temperatures, erratic power supplies, and dust entering the system (20).

1.3 Diagnostics Based on Polymerase Chain Reaction Require a Controlled Environment

The Polymerase Chain Reaction (PCR), a Nobel Prize-winning development by Kary Mullis (21), is the exponential amplification of double-stranded DNA by cycling between an optimized hot temperature and cooler temperature. As the system heats up, the double-stranded DNA melts apart into two complementary strands; as it cools, primers anneal on these strands, allowing DNA polymerase to bind and begin creating a new complementary strand with dNTPs (deoxyribonucleotide triphosphates, building blocks of DNA) present in the reaction. Therefore, the number of copies of the DNA target in the reaction doubles every cycle, creating exponential amplification. Because these primers are specific to the DNA sequence for which the assay is testing, amplification will only occur if that sequence is present in the reaction.

Successful amplification was originally determined through gel electrophoresis by looking for DNA fragments of the correct size. The first real-time quantitative PCR instruments and assays were developed in 1996 using either dyes such as SYBR Green that fluoresce when bound to double-stranded DNA or fluorophore-labelled probes to quantify the amount of DNA template present in the reaction without requiring post-PCR sample handling (22). This method both decreases the time required and improves the specificity of the assay, as the probe must bind to a specific sequence within the target amplicon to fluoresce. The previously-mentioned GeneXpert device is based on this method.

Quantitative PCR works well with viruses that store their genetic code as DNA, such as chickenpox and herpes, but not for those with RNA, like dengue, Zika, and chikungunya. RNA must be reverse-transcribed into the complementary DNA strand (cDNA) to be amplified by PCR. Reverse Transcriptase, also a Nobel Prize-winning development, was found within RNA tumor viruses, or viruses that can cause cancer, and was commercialized and employed to convert RNA into complementary DNA (cDNA) during a short hold time at a specific temperature (23). Most standard-model PCR machines can be programmed to include a reverse transcription (RT) step before thermal cycling, but without availability of these machines in the developing world, this high-capability diagnostic technique is unavailable.

Current PCR machines depend entirely on accurate control of the temperature of the reaction over long periods of time. Precise temperature control is crucial for achieving the conditions required to melt double stranded DNA or anneal primers to target strands; without this control, amplification could be prevented despite presence of the target sequence. In programming PCR machines, technicians assume the double- or single-stranded state of the nucleic acids at specific temperatures. Contaminants in the reaction, such as ethanol used in extraction procedures, human serum, and salts found in urine, can alter that state. The requirements of consistent machine calibration and laboratory-purified samples preclude the widespread use of PCR in the developing world, where a simple and robust PCR technology would be highly beneficial.

1.4 Adaptive PCR and its Limitations in Reverse Transcription Reactions

In order to combat the difficulties in PCR diagnostics at the point-of-care mentioned above, we have created a real-time PCR technique that does not require direct temperature sensing or optimization (24). Instead of heating and cooling the sample to optimized temperature points and

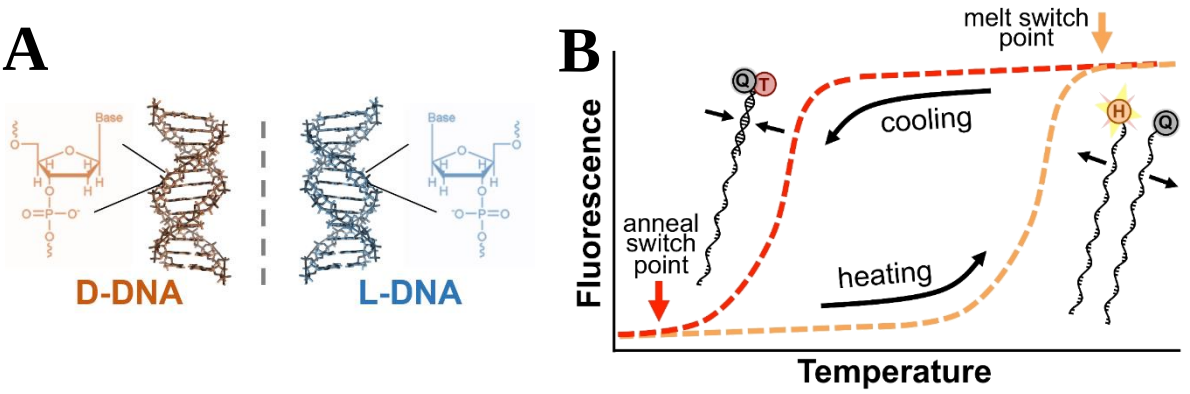

***Figure 1**: Illustration of L-DNA and Adaptive PCR.* **(A)** Left-handed DNA is the enantiomer, or mirror image, of right-handed D-DNA. **(B)** Control of Adaptive PCR through L-DNA monitoring. During heating (yellow), the HEX channel is used to monitor the template strand melting. During cooling (red), the Texas Red channel is used to monitor annealing of the primers. From Adams, et al. (24).

assuming the state of the DNA, Adaptive PCR infers the state of the oligonucleotide molecules instantaneously using left-handed DNA, or L-DNA. L-DNA is the enantiomer of naturally-occurring D-DNA (**Figure 1A**); it does not occur naturally and does not interact with its right-handed counterpart or with DNA polymerase (25, 26). In this approach, the addition of fluorescently-labelled strands of L-DNA that correspond to the primers used to amplify the D-DNA target allow the melting and annealing states of the DNA to be monitored (**Figure 1B**). We refer to these L-DNA strands as L-DNA melt indicator probes and L-DNA primer anneal indicator probes.

In the first iteration of Adaptive PCR (24), the L-DNA probes were designed to be identical to the primer and target sequences for *Mycobacterium tuberculosis* used in the assay. The melt probe was designed with the long target sequence with the HEX fluorophore conjugated to the 5' end; a reverse version of this probe was designed with a 3' Black Hole Quencher (BHQ) dye to suppress the HEX signal when the two are bound. The anneal probe used the primer sequence from the assay with a Texas Red fluorophore conjugated to the 5' end; when this primer annealed to the reverse target, the BHQ quenches the Texas Red, causing a decrease in fluorescence. The Texas

Red anneal probe and the BHQ target probe were added to the reactions at 100 nM with 20 nM of the HEX melt probe.

A fluorescence detector is used to monitor the L-DNA melt and anneal indicators in the reaction, which then communicates through a LabVIEW program to a heating element (**Figure 2**). By controlling the reaction based on the actual state of the DNA, Adaptive PCR achieves optimum thermal cycling even if the sample contains unexpected background contaminants.

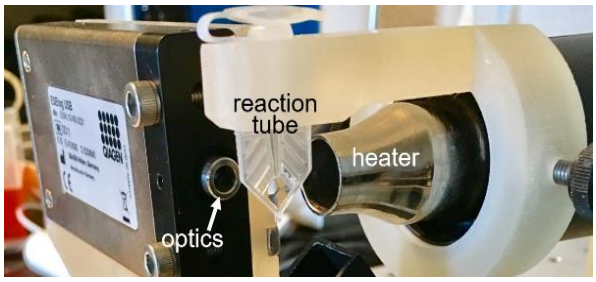

***Figure 2**: The Current Adaptive PCR Prototype.* The optical device (Qiagen ESELog) emits and detects fluorescence signal and communicates with LabVIEW via USB connection. The heater and fan are connected through a relay circuit and can be cycled on and off by the program based on the signal received from the optics. Further detail can be found in Adams, et al. 2016 (24).

1.5 Adaptive PCR Must Be Modified for Multiplexed Detection of Viral RNA

To address the needs of RNA virus diagnostics, there are several modifications that must be made to Adaptive PCR. In the first iteration (24), the system was designed to monitor the annealing and melting steps of a PCR reaction and did not incorporate the reverse transcription step required for RNA detection. The system also did not have the capability to do multiplex nucleic acid target identification. Reverse transcription requires some form of temperature monitoring for the 10-minute temperature hold time, and multiplexing targets requires additional fluorescence channels and compatible assay designs. Incorporating an optics-based method for reverse transcription temperature control, creating a method for incorporating multiple fluorescence channels, and developing compatible primer and probe designs for multiplexed reactions is the basis of this report and has resulted in the production of a robust device for detecting and differentiating three RNA viruses in a single reaction tube.

2: METHODS

2.1 Oligonucleotide Design

Purified genomic Zika RNA (prod. no. VR-1838DQ™) and synthetic RNA genomes for chikungunya (prod. no. VR-3246SD™) and dengue (prod. no. VR-3228SD™) were purchased from the American Type Culture Collection (ATCC). Primers and hydrolysis probe sequences for each were identified from previous studies and purchased from Integrated DNA Technologies (**Table 1**). The dengue sequences were selected based on ATCC recommendation, which directly references an assay published by the CDC (27). The Zika sequences are also from CDC documentation (28). The chikungunya primer and probe sequences were also recommended by ATCC for the genomic RNA we purchased from them (Note: ATCC attributes the sequences to the Liverpool School of Tropical Medicine, but we were unable to find documentation of the source of these sequences).

***Table 1**: Oligonucleotide Sequences*

D-DNA	CHIKV F Primer	5'-TACAGGGCTCATACCGCATC
	CHIKV R Primer	5'-AAAGGTGTCCAGGCTGAAGA
	CHIKV Probe	5'-**Cy5**-CGACCATGCCGTCACAGTTAAGGA-**BHQ2**
	DENV F Primer	5'-CAAAAGGAAGTCGYGCAATA
	DENV R Primer	5'-CTGAGTGAATTCTCTCTGCTRAAC
	DENV Probe	5'-**HEX**-CATGTGGYTGGGAGCRCGC-**BHQ1**
	ZIKV F Primer	5'-CAGCTGGCATCATGAAGAAYC
	ZIKV R Primer	5'-CACCTGTCCCATCTTTTTCTCC
	ZIKV Probe	5'-**FAM**-CYGTTGTGGATGGAATAGTGG-**BHQ1**
L-DNA	RT Molecular Beacon	5'-**FAM**-GCGAGAAAAAAAAAAAAAAACTCGC-**BHQ2**
	Anneal Indicator Probe	5'- **TEX**-CAGCTGGCATCATGAAGAATC
	Anneal Indicator Compl	5'-GATTCTTCATGATGCCAGCTG-**BHQ2**
	Melt Indicator Probe	5'-**TEX**-CTTTGTCACCGACGCCTACGTCGCAGGATCCTGGGCTGGCGGG TCGCTTCCACGATGGCCACCTCCATGGTCCTCGA
	Melt Indicator Compl	5'-TCGAGGACCATGGAGGTGGCCATCGTGGAAGCGACCCGCCAGCCCA GGATCCTGCGACGTAGGCGTCGGTGACAAAG-**BHQ2**

L-DNA primer anneal indicator probes were designed with sequences identical to the Zika primers, with 5'-Texas Red dye on the forward primer and 3'-Black Hole Quencher 2 (BHQ2) dye on the reverse primer. We chose target melt probes from a previous tuberculosis (TB) assay performed by our lab because the Zika target sequence was longer than could be effectively synthesized as L-DNA and we had shown that the GC-rich TB sequence melted at a suitable temperature for all three viruses (approximately 92°C). A molecular beacon was designed to hold at approximately 50°C for the RT step based on a report of thermal sensitivity in relation to sequence length (29), although the poly-T loop sequence was switched for poly-A to avoid binding with the poly-A tail of mRNA in the preliminary D-DNA design. All L-DNA probes were purchased from Biomers.net GmbH (Ulm, Germany).

2.2 LabVIEW Reverse Transcription Program

The molecular beacon was designed with a quencher and fluorophore on each end, so that as the temperature increases through the desired T_M of 50°C, the hairpin melts apart and the fluorescence increases in a sigmoidal curve (see Section 3.1). LabVIEW then uses the same fitting program as in cycling to fit the derivative of this curve and find the point of greatest slope. Monitoring the beacon's fluorescence at the point where it varies most significantly with temperature allows for detection of small temperature fluctuations and therefore fine control of the heating element. The LabVIEW system was programmed to turn the heater on and off as necessary to keep the instantaneous fluorescence value as close to this "set point" as possible: to turn the heater on if the fluorescence value is below the desired value and to turn it off if the fluorescence value is too high. After the prescribed hold time, the system was programmed to transition into Adaptive PCR cycling, as previously reported (24).

To confirm efficacy, a thermocouple was inserted into the reaction volume to monitor temperature during a hold. The temperature hold was tested seven times over three days to ensure consistency of the system's decision-making and temperature range (see Section 3.1).

2.3 Single Fluorescence Channel Heating and Cooling Program

To allow three of the four available fluorescence channels on the Adaptive PCR instrument to be used for amplification detection, both the anneal and melt L-DNA probes were measured on the same color channel. Texas Red was chosen due to its thermal stability, i.e. that its fluorescence signal varies minimally with temperature (30). As the L-DNA anneal probe melts approximately 25°C before the melt probe, the plateau of Texas Red fluorescence during heating from anneal probe melting occurs before the signal from melt probe melting starts to interfere (see Section 3.2). Therefore, the two plateaus are distinct from each other and can be distinguished by the program using a Gaussian fit, as in the original iteration of Adaptive PCR (24). After the first plateau is found, the program ignores the heating data from before that point to fit the second plateau separately, followed by a transition to the cooling state. The same progression is employed during the cooling cycle – LabVIEW fits data from the first plateau, that of the melt probe annealing, and then ignores it so that it fits the second, more important, plateau, which indicates the anneal probe annealing.

2.4 LabVIEW Multiplex Program

The original Adaptive PCR cycling program was altered to allow for multiple PCR target fluorophores to be detected simultaneously. Depending on which channels are set to "ON", the Qiagen ESELog devices will detect the selected colors in order and record points within up to three

different PCR files. Different fluorophores were selected for each of the three probes used in the chikungunya, dengue, and Zika assay so that they can all be detected separately within the reaction.

2.5 Limit of Detection of RNA Targets on Adaptive RT-PCR

Each of the synthetic genomic RNA targets were tested at 10^3, 10^2, 10^1, and 10^0 copies/µL in triplicate at 5µL per 25µL reaction, correlating to 5,000, 500, 50, and 5 RNA copies per reaction, respectively. "No Template Controls" (NTCs) with water instead of RNA were also tested as negative controls. Triplicate trials were also conducted with pairs of targets and with all three targets, each at 50 copies per reaction. Data from triplicate trials were averaged and normalized by fitting the fluorescence values to a 0-100 unit scale.

The BioLine SensiFAST^{TM} Probe No-ROX One-Step Kit was used for all reactions according to their protocol. All D-DNA primers (6) and probes (3) were included in each reaction at 0.4µM (**Table 1**). The FAM-conjugated molecular beacon was added at 10 nM. The L-DNA probes were each added at 50 nM and the L-DNA complements were added at 125 nM. Relative concentrations were selected in order to create derivatives of fluorescence signal at approximately the same magnitude so that neither the anneal or melt probe signal could bleed into or overpower the other.

3: RESULTS AND DISCUSSION

3.1 Optically-Controlled Reverse Transcription Step

Reverse Transcription reactions are required to transcribe RNA into double-stranded complementary DNA (cDNA) prior to PCR amplification. Current Reverse Transcription PCR (RT-PCR) kits require a 10-minute hold at a constant temperature, most often between 45-60°C. Because Adaptive PCR does not include temperature sensing, it did not have the capacity to perform this step. To incorporate this functionality, a program was developed based around the fluorescence signal of a temperature-sensitive molecular beacon (**Figure 3**).

Molecular beacons are hairpin strands of DNA that emit fluorescence signal as a function of temperature (**Figure 3A**). Previously used to detect intracellular temperatures (29, 31), the number of base pairs in the hairpin of the beacon determine the temperature at which it melts and therefore fluoresces. Because most commercial reverse transcription kits require a hold temperature between 45-60°C, a sequence was designed so that the greatest change in fluorescence per change in temperature fell in the middle of that range, i.e. between 50-55°C (**Figure 3B**).

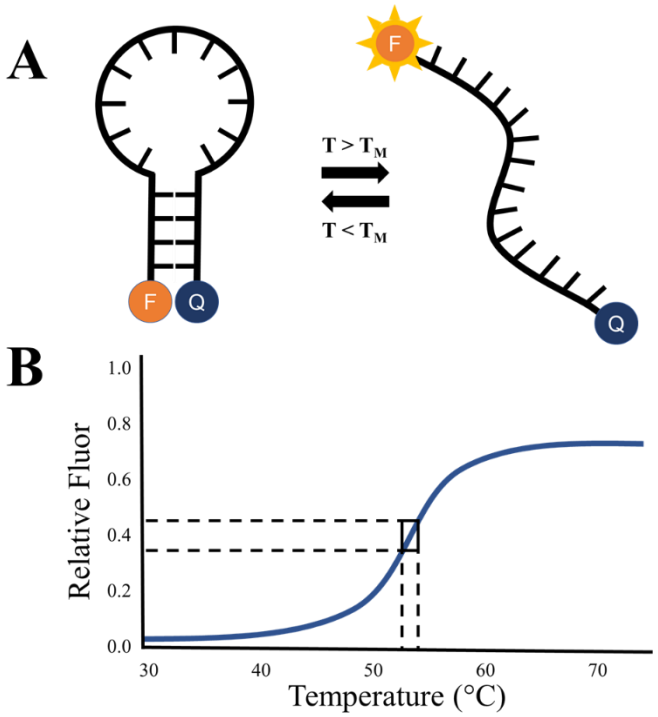

Figure 3: *Molecular Beacons for Temperature Holding.* **(A)** An illustration of a molecular beacon hairpin with a fluorophore (F) and quencher (Q) on opposite ends. **(B)** A graphical illustration of the fluorescence signal from a molecular beacon in response to temperature. The Adaptive PCR program keeps the fluorescence between the horizontal dotted lines so that the temperature remains in the range of the corresponding vertical lines. Adapted from Ke, et al. (29).

All molecular beacon sequences from Ke, et al. (29) contain a poly-T sequence at the center to make up the hairpin loop, but as mature mRNA contains a poly-A tail that could bind to this poly-T region, the preliminary D-DNA beacon was adapted to include a poly-A central sequence (**Table 1**); the L-DNA version was then designed with an identical sequence to the D-DNA beacon.

Originally, we conjugated Texas Red to the beacon to allow all three L-DNA probes (melt, anneal, and RT) to operate within the same channel. However, the fluorescence inclines and plateaus of the melting of the molecular beacon and the melting of the L-DNA primer sequences overlapped too much, preventing differential signal detection. The same sequence was therefore redesigned with FAM conjugated instead. While this is the same as the fluorophore conjugated to the Zika probe, the concentration of the molecular beacon is low enough that the signal is negligible relative to the signal produced by Zika amplification.

Using the same Gaussian fit program as in thermal cycling, the LabVIEW code was designed to find the point of greatest derivative in fluorescence and then to keep the instantaneous fluorescence value as close to that point as possible. If the fluorescence is above the ideal value, the heater turns off; as the fluorescence descends below the value, the heater turns back on. This continues for ten minutes, at which point the system transitions into PCR thermal cycling.

To confirm the accuracy of the molecular beacon-based hold step, a thermocouple was inserted into the reaction tube for seven 30-minute hold trials (**Figure 4**). Although most Reverse Transcription kits only require 10 minutes of hold time, 30-minute trials were conducted to confirm that it was stable over longer periods of time. Sufficient thermal stability was shown in all trials, with averages of each trial ranging from 50-53.5°C and intra-trial standard deviations of ~0.5°C. The variability in temperature averages seen in **Figure 4** are believed to be due to slightly different data interpretations by the LabVIEW program; the system records a new data point every 0.33

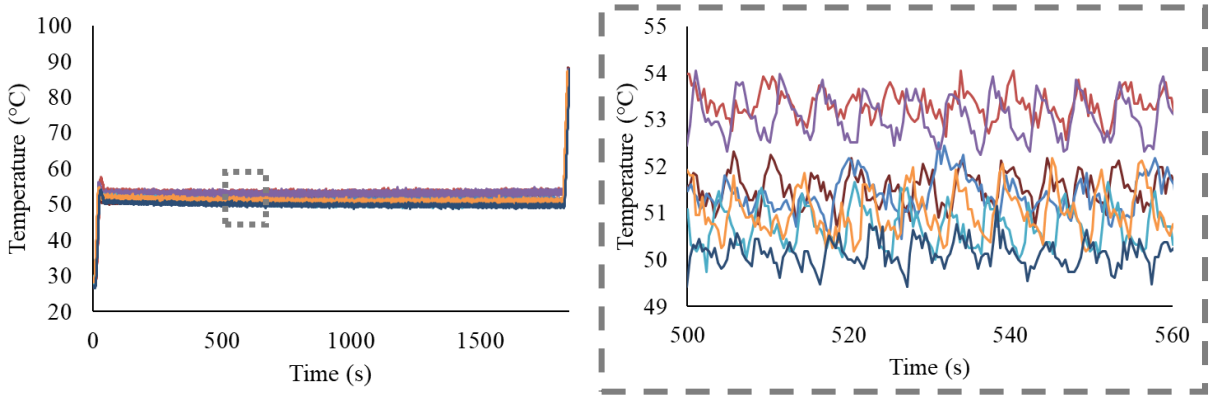

***Figure 4**: Thermocouple-Monitored Molecular Beacon Holds.* Seven 30-minute trials of reverse transcription temperature holds by the Adaptive PCR instrument using the molecular beacon indicator. The larger graph shows the full 30 minutes, including less than one minute on each end to show initial fitting and transition into cycling. The zoomed-in graph shows intra-trial variation during a one-minute period.

seconds, so a difference in one or two data points required to determine the "set point" can cause it to cycle around a slightly higher temperature, as time is directly related to the amount of heat delivered. Over the 60 seconds shown in the inset of **Figure 4**, the number of heat/cool cycles varied from about 10-12. The periodicity of the temperature data is a result of the control mechanism – the system switches between heating and cooling periodically as the fluorescence value fluctuates. The amount of time required to cool below the fluorescence set point is directly related to the ambient temperature in the room, as the cooling state is the absence of the heater. It would therefore require more time to cool in tropical environments. Reverse transcriptase requires only that the temperature remain between 45-60°C which is consistently achieved through this method.

3.2 Single-Channel Cycling and Multiplex PCR

Multiplex PCR allows for the simultaneous detection of several different DNA targets, each with different fluorophore combinations. The current Adaptive PCR device has the capability of detecting four different fluorophores, two from each Qiagen ESELog: HEX, Texas Red, FAM, and Cy5. In the earlier iteration of Adaptive PCR (24), HEX dye was conjugated to the melt L-

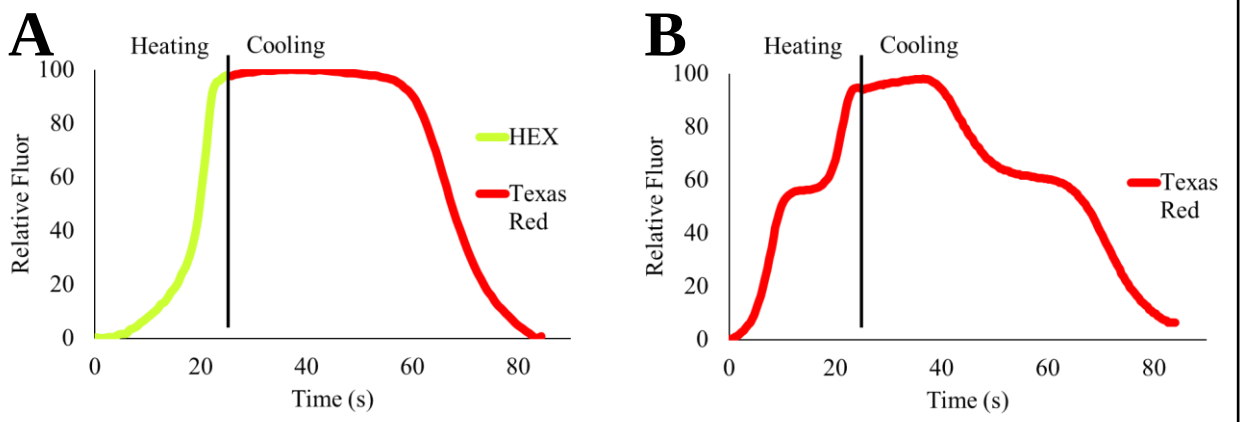

***Figure 5**: Fluorescence as a Function of Time for Double- vs. Single-Channel Cycling.* **(A)** The original, two-fluorophore Adaptive PCR system. The yellow color represents HEX, the fluorophore monitored during heating; red represents Texas Red, the color monitored during cooling. This graph is an analog of the information shown in **Figure 1B**. **(B)** The new single-fluorophore Adaptive PCR system. The middle plateau on each part of the cycle represents the melting of the primers and the annealing of the template strands. Because these occur at very different temperatures, the two plateaus can clearly be distinguished during the Gaussian fit program in LabVIEW. In both versions, cooling takes much longer than heating because it heats actively (via heat gun) but cools passively.

DNA probe and Texas Red dye to the anneal L-DNA probe (**Figure 5A**). However, this required the use of two of the four available channels for thermal cycling. In order to "free up" another of those channels for PCR amplification detection, a new switching program was designed to allow Texas Red dye to be used on both the anneal and melt L-DNA probes (**Figure 5B**).

The L-DNA anneal probe was designed to match the Zika primer sequence and its complement. Because the Zika target sequence was too long to be effectively synthesized as L-DNA, a suitable template sequence and its complement from a previous Adaptive PCR assay were used for the L-DNA melt probe. The two probes can be monitored on the same channel because the melt and annealing points of the primers (~60°C) and the targets (~87°C) are distinct, and the melt and annealing curves do not overlap (**Figure 5B**). Interestingly, melt and annealing curves were initially slightly more difficult to distinguish during the cooling phase of the cycle. This seemed to be the result of the slower kinetics of annealing, which relies on diffusion for the two oligonucleotides to bind. The slow kinetics during cooling caused the annealing curve of the melt probe to extend and overlap with the annealing curve of the anneal probe, which made it difficult

for the program to accurately identify the anneal point of the primers. To resolve this issue, some adjustments were made. The concentrations of the melt and anneal probes were optimized to ensure equal signal was detected from each. Also, the LabVIEW program was altered to reduce the constraints for finding a Gaussian fit.

The remaining three channels were then used for detection of the three PCR targets. FAM was used to label the Zika probe, HEX was used to label the dengue probe, and Cy5 was used to label the chikungunya probe. The LabVIEW program triggers the Qiagen ESELog devices to detect from each of the three channels at the end of each cooling cycle, plotting the data from each channel on separate graphs.

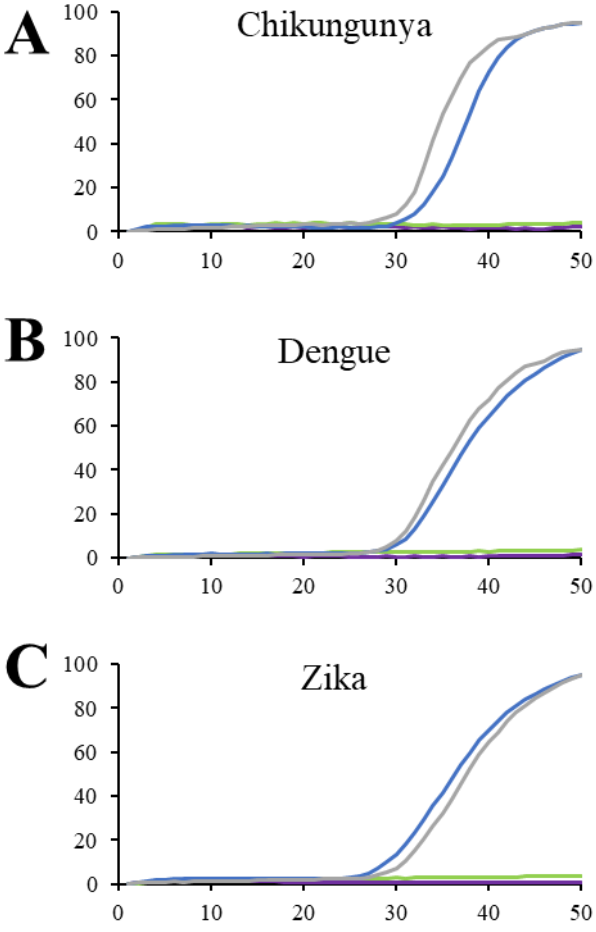

***Figure 6**: Comparison of RotorGene and Adaptive PCR.* Each of the RNA virus targets were tested at 5,000 copies/reaction in both the RotorGene and Adaptive PCR. The RotorGene data (gray) and the Adaptive PCR data (blue) amplified at approximately the same C_T. None of the "No Template Control" (NTC) trials amplified on either RotorGene (green) or Adaptive PCR (purple).

To confirm efficacy of the assay design, each of the three viruses was tested at 10^3 copies/µL with 5 µL of sample in the reaction (5,000 copies/reaction) in both a Qiagen Rotor-Gene Q 5-plex HRM instrument and on Adaptive PCR (**Figure 6**). The amplification curves of both instruments appear similar for each virus. The threshold cycle (C_T), or the cycle at which the amplification curve passes the threshold and begins to visibly increase, for both instruments is within one cycle for each of the viruses. This variation is likely due to minor trial-by-trial variability and would appear equivalent with a greater number

of trials performed. In conducting these tests, we also confirmed that none of the negative controls amplified, showing that the assay does not misidentify any of the viruses as another.

3.3 Limit of Detection of the Chikungunya, Dengue, and Zika Assay

The limit of detection of each target was then tested (**Figure 7**). Chikungunya virus concentrations were distinguishable down to 5 copies/reaction, and the cycle number at which each concentration begins to amplify (C_T) follows a normal pattern (**Figure 7A**). The average viral load mentioned previously was on the order of 100 RNA copies per µL of patient sample (500 copies/reaction, orange curve) for symptomatic patients and 1 copy per µL (5 copies/reaction, yellow curve) for asymptomatic patients (7); this assay detects both concentrations accurately. A dengue viral load of 1 copy per µL was considered "very low" (17) and was not detectable by this assay, but the RNA was distinguishable down to 10 copies/µL (**Figure 7B**). Each of the concentrations of Zika virus was cleanly distinguishable from the others (**Figure 7C**), meaning that the viral loads of 10 copies/µL of blood and 1 copy/µL of serum (18) are both detectable.

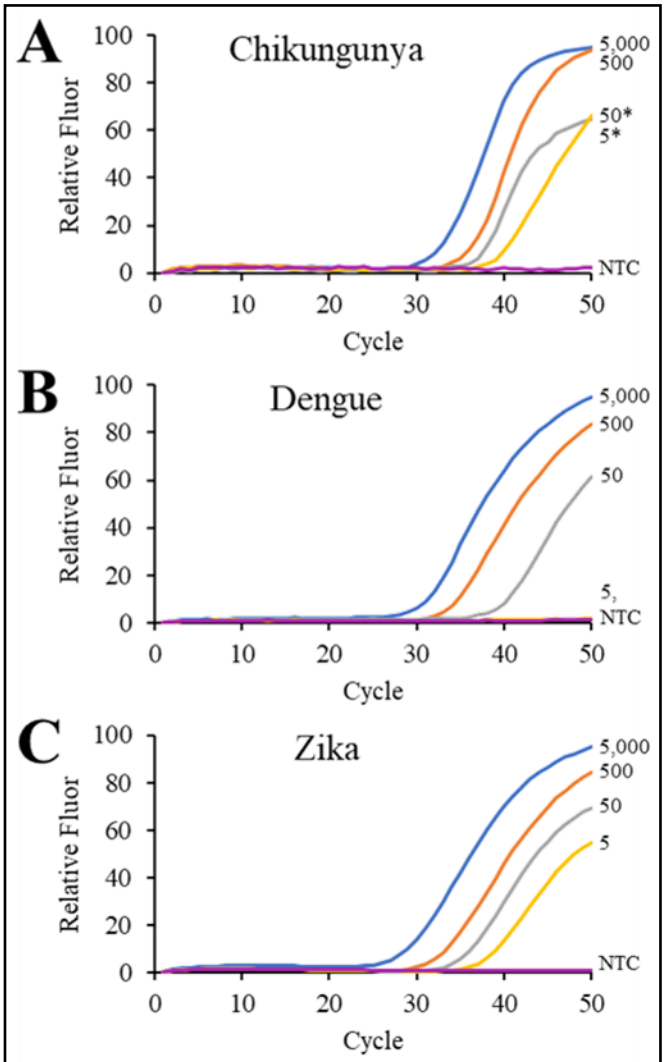

***Figure 7**: Limit of Detection of Chikungunya, Dengue, and Zika Viruses.* All concentrations of each virus were conducted in triplicate and averaged. **(A)** The standard curve for chikungunya. **(B)** The standard curve for dengue. **(C)** The standard curve for Zika. *n=2

3.4 Multiplexed Reaction Specificity

Because 50 copies/reaction was the lowest concentration consistently detectable in all three targets, that concentration was used to test detection of combinations of targets (**Figure 8**). All three viruses were amplified within one cycle in combination with either or both of the other targets. In two particular combinations, amplification efficiencies were slightly decreased: Zika in the presence of dengue (gray and yellow curves in **Figure 8C**) and dengue in the presence of chikungunya or Zika (orange, gray, and yellow curves in **Figure 8B**). This is possibly due to competition between the different RNA or cDNA for the primers; if the dengue primers can bind with low affinity to part of the Zika target, for example, that reduces the number of primers available for dengue amplification. In practice, these reduced efficiencies will have little impact, particularly because the likelihood of a patient having co-infections of these viruses is relatively low.

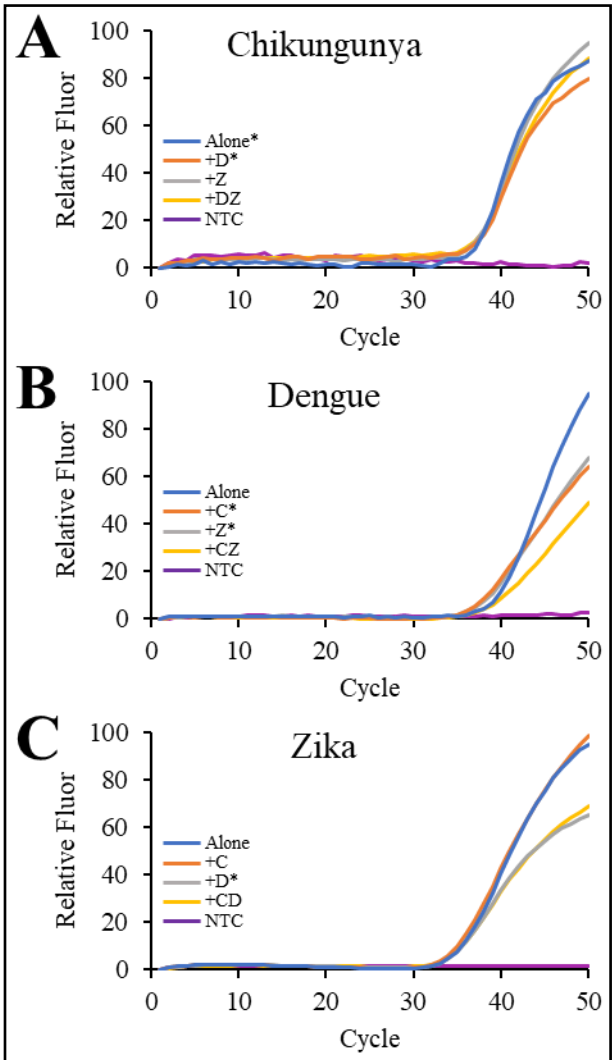

***Figure 8**: Amplification of PCR Targets In Combination at 50 Copies/Reaction.* **(A)** Amplification of chikungunya virus in the presence of equal amounts of dengue (orange), Zika (gray), and both (yellow). **(B)** Amplification of dengue virus in the presence of chikungunya (orange), Zika (gray), and both (yellow). **(C)** Amplification of Zika virus in the presence of chikungunya (orange), dengue (gray), and both (yellow). *n=2

4: CONCLUSIONS

This work has resulted in the development of an assay for the Adaptive PCR system to detect the presence of the viral genome of chikungunya, dengue, and Zika viruses in the reaction down to 5 (chikungunya, Zika) or 50 (dengue) copies per reaction. The concentrations at which this assay detects each of the three viruses are clinically relevant for existing viral loads mentioned previously (7, 17, 18): samples from the average patient infected with one of these viruses can be diagnosed using this assay. Our method for optically-based reverse transcription gave stable temperature holds and successful reverse transcriptase activity. Multiplexing was specific to each of the three targets, as there was no visible amplification of negative controls. The Adaptive RT-PCR device equipped with this assay has the potential to be immensely useful in the developing world to diagnose these infections, and the system can be easily adjusted to test for other nucleic acid sequences and for other virus groups as well.

5: FUTURE DIRECTIONS

As mentioned previously, the WHO's ASSURED criteria can be used to determine usability of a device in these environments: affordable, sensitive, specific, user-friendly, rapid and robust, equipment-free, and deliverable to end users (15). While this work establishes the sensitivity and specificity of the Adaptive PCR system for RNA viruses, there is still much to be done to reach the other milestones.

5.1 Affordable

The affordability of the device and the assays it can perform will be greatly improved by developing a device with non-OEM parts and by mass production of assay components. This device must primarily replace the expensive Qiagen ESELog fluorescence detector components in favor of much less expensive LEDs and photodetectors in conjunction with light filters, all of which are incorporated within the Qiagen ESELog. The assays themselves will become less expensive when individual components, such as L-DNA probes, are ordered and combined in bulk; it is estimated that each reaction will cost approximately $0.01. Bulk ordering will be a viable solution once the device has been shown to meet the other criteria in the desired settings.

5.2 User-Friendly

The usability of the Adaptive PCR system must be improved through further development of a simpler user interface. The current LabVIEW system contains many troubleshooting mechanisms that are confusing to the untrained user. The technician at the point-of-care should be able to select an assay within an integrated User Interface, preferably from a connected tablet or

something similar, and simply press “Run.” This capability has been partially developed for the assay developed in this work.

We have also performed some preliminary testing in using a lyophilizable RT-PCR kit, in which a master mix of all necessary reagents can be produced and separated into individual reaction volumes, then freeze-dried until use. These tubes then only need to be rehydrated with the desired patient sample and inserted into the Adaptive PCR device. This would also increase usability as almost all pipetting requirements would be removed.

5.3 Rapid and Robust

The Adaptive PCR system is more robust than standard PCR, as it overcomes challenges from several contaminants known to inhibit proper thermal cycling (24). However, this could be improved through further testing and optimization on patient samples such as blood and urine. Some preliminary tests using human serum have delivered promising results.

The speed of the assay could be greatly improved through incorporation of a different reaction tube. Preliminary testing on several types of capillary tube showed proper signal detection through much faster cycling times, likely due to an increased thermal diffusion rate through a larger surface area:volume ratio. However, the speed of the reaction was accompanied by imprecise detection of anneal and melt states, decreasing consistency and efficiency of the reaction. Further testing on similar mechanisms is needed to develop a rapid assay.

5.4 Equipment-Free and Deliverable

The improvement of the device to be smaller and more portable will accomplish both of the last two ASSURED criteria. While the device is itself “equipment,” it will be small and will

achieve the main idea of the “equipment-free” criterion – that several parts and pieces are not required and that it is battery-powered. The device is projected to be about the size of a shoebox and contain a slot mechanism for insertion of the reaction tube. Clinics in low-resource environments need only have a stock of lyophilized reactions for each of the desired tests and a device with which they can select the test they wish to perform, insert the sample, and press “Run.” Such a system would be deliverable to the desired groups with some external funding and would greatly increase the standard of diagnostic care for people in low-resource environments.

REFERENCES

1. Saeed MA & Attia TH (1992) Dengue and Dengue Hemorrhagic Fever. *Afro-Egypt J Infect Endem Dis*.

2. WHO (2017) Dengue and Severe Dengue. (World Health Organization).

3. CDC (2012) Dengue Virus - What to Do if You Think You Have Dengue. (Centers for Disease Control and Prevention).

4. CDC (2017) Zika Virus - Symptoms, Testing, and Treatment. (Centers for Disease Control and Prevention).

5. Oliveira Melo AS, *et al.* (2016) Zika Virus Intrauterine Infection Causes Fetal Brain Abnormality and Microcephaly: Tip of the Iceberg? *Ultrasound in Obstetrics & Gynecology* 47(1):6-7.

6. CDC (2016) Chikungunya Virus - Symptoms, Diagnosis, and Treatment. (Centers for Disease Control and Prevention).

7. Appassakij H, Khuntikij P, Kemapunmanus M, Wutthanarungsan R, & Silpapojakul K (2013) Viremic Profiles in Asymptomatic and Symptomatic Chikungunya Fever: a Blood Transfusion Threat? *Transfusion* 53(10pt2):2567-2574.

8. Pabbaraju K, *et al.* (2016) Simultaneous Detection of Zika, Chikungunya and Dengue Viruses by a Multiplex Real-Time RT-PCR Assay. *Journal of Clinical Virology* 83:66-71.

9. Rajapakse S (2011) Dengue Shock. *Journal of Emergencies, Trauma and Shock* 4(1):120-127.

10. Furuya-Kanamori L, *et al.* (2016) Co-Distribution and Co-Infection of Chikungunya and Dengue Viruses. *BMC Infectious Diseases* 16(1):84.

11. Villamil-Gómez WE, González-Camargo O, Rodriguez-Ayubi J, Zapata-Serpa D, & Rodriguez-Morales AJ (2016) Dengue, Chikungunya and Zika Co-Infection in a Patient from Colombia. *Journal of Infection and Public Health* 9(5):684-686.

12. Tang Y-W, Procop GW, & Persing DH (1997) Molecular Diagnostics of Infectious Diseases. *Clinical Chemistry* 43(11):2021.

13. Petti CA, Polage CR, Quinn TC, Ronald AR, & Sande MA (2006) Laboratory Medicine in Africa: A Barrier to Effective Health Care. *Clinical Infectious Diseases* 42(3):377-382.

14. McNerney R (2015) Diagnostics for Developing Countries. *Diagnostics* 5(2):200-209.

15. Wu G & Zaman MH (2012) Low-Cost Tools for Diagnosing and Monitoring HIV Infection in Low-Resource Settings. (World Health Organization), pp 914-920.

16. CDC (2017) Diagnostic Tests for Zika Virus. (Centers for Disease Control and Prevention).

17. Laue T, Emmerich P, & Schmitz H (1999) Detection of Dengue Virus RNA in Patients after Primary or Secondary Dengue Infection by Using the TaqMan Automated Amplification System. *Journal of Clinical Microbiology* 37(8):2543-2547.

18. Corman VM, *et al.* (2016) Assay Optimization for Molecular Detection of Zika Virus. *Bulletin of the World Health Organization* 94(12):880.

19. Weidemaier K, Carrino J, Curry A, Connor JH, & Liebmann-Vinson A (2015) Advancing Rapid Point-of-Care Viral Diagnostics to a Clinical Setting. *Future Virology* 10(3):313-328.

20. Creswell J, *et al.* (2014) Results from Early Programmatic Implementation of Xpert MTB/RIF Testing in Nine Countries. *BMC Infectious Diseases* 14:2-2.

21. Mullis KB (1987) Process for Amplifying Nucleic Acid Sequences. (US Patent 4,683,202).

22. Heid CA, Stevens J, Livak KJ, & Williams PM (1996) Real-Time Quantitative PCR. *Genome Research* 6(10):986-994.

23. Goff SP (1990) Retroviral Reverse Transcriptase: Synthesis, Structure, and Function. *JAIDS Journal of Acquired Immune Deficiency Syndromes* 3(8).

24. Adams NM, Gabella WE, Hardcastle AN, & Haselton FR (2016) Adaptive PCR Based on Hybridization Sensing of Mirror-Image L-DNA. *Analytical Chemistry* 89(1):728-735.

25. Garbesi A, *et al.* (1998) Chirally-Modifiedoligonucleotides and the Control of Gene Expression. The Case of L-DNAS And-RNAS. *Nucleosides & Nucleotides* 17(7):1275-1287.

26. Anderson DJ, Reischer RJ, Taylor AJ, & Wechter WJ (1984) Preparation and Characterization of Oligonucleotides of D-and L-2'Deoxyuridine. *Nucleosides & Nucleotides* 3(5):499-512.

27. CDC (DENV-1-4 Real-Time RT-PCR Assay for Detection and Serotype Identification of Dengue Virus. Instructions for Use Package Insert. (Centers for Disease Control and Prevention).

28. Jesse JW, *et al.* (2016) Single-Reaction Multiplex Reverse Transcription PCR for Detection of Zika, Chikungunya, and Dengue Viruses. *Emerging Infectious Disease Journal* 22(7):1295.

29. Ke G, *et al.* (2012) L-DNA Molecular Beacon: a Safe, Stable, and Accurate Intracellular Nano-Thermometer for Temperature Sensing in Living Cells. *Journal of the American Chemical Society* 134(46):18908-18911.

30. You Y, Tataurov AV, & Owczarzy R (2011) Measuring Thermodynamic Details of DNA Hybridization Using Fluorescence. *Biopolymers* 95(7):472-486.

31. Kim Y, Yang CJ, & Tan W (2007) Superior Structure Stability and Selectivity of Hairpin Nucleic Acid Probes with an L-DNA Stem. *Nucleic Acids Research* 35(21):7279-7287.

APPENDIX

All data can be found in the Haselton Lab Dropbox in the folders Gates Phase 1.5 > Temperature Probes > Data > Adaptive RT-PCR CDZ Data (Erin's Thesis). Each data file contains the information listed below:

CHIKV Amplification (Adaptive PCR)

10^3 copies/µL: 20180205_161218
20180205_172307
20180206_113246
10^2 copies/µL: 20180208_114058
20180208_140721
20180302_135515
10^1 copies/µL: 20180222_131519
20180222_145916
10^0 copies/µL: 20180222_163119
20180223_115455

DENV Amplification (Adaptive PCR)

10^3 copies/µL: 20180130_165130
20180131_103617
20180201_133500
10^2 copies/µL: 20180130_123831
20180130_183337
20180201_122043
10^1 copies/µL: 20180214_113658
20180214_153046
20180214_175636
10^0 copies/µL: 20180214_141951
20180214_164655
20180215_102435

ZIKV Amplification (Adaptive PCR)

10^3 copies/µL: 20180118_112140
20180213_142425
20180213_162638
10^2 copies/µL: 20180202_124059
20180213_124118
20180223_152010
10^1 copies/µL: 20180202_112934
20180213_110856
20180223_163641
10^0 copies/µL: 20180212_155722
20180212_144859
20180223_175314

No Template Control (Adaptive PCR)

20180122_143702
20180208_123353
20180226_165914

CHIKV 10^1 + DENV 10^1 (Adaptive PCR)

20180227_144044
20180227_171217

CHIKV 10^1 + ZIKV 10^1 (Adaptive PCR)

20180228_142938
20180228_153924
20180228_165550

DENV 10^1 + ZIKV 10^1 (Adaptive PCR)

20180227_105842
20180227_131957

CHIKV 10^1 + DENV 10^1 + ZIKV 10^1
(Adaptive PCR)
20180228_105509
20180228_122506
20180228_181841

Temperature Hold Data
20171103_153918
20171103_163128
20171106_132615
20171106_142811
20171106_150854
20171113_123234
20171113_141006

RotorGene Data
Run 2018-03-15 everything for paper

Excel Analysis Sheets
171103 Temperature Hold Data
RotorGene Adaptive Compare
LOD Data

Figures (PowerPoint)
Paper Figures and Necessary Data